Available online at www.sciencedirect.com
SCIENCE DIRECT®
Polyhedron 24 (2005) 2346–2349
POLYHEDRON
www.elsevier.com/locate/poly

^{55}Mn NMR spectra of Mn_{12} single-molecule magnets: Single crystal versus aligned powder studies

A.G. Harter [a], N.E. Chakov [b], R. Achey [a], A. Reyes [a], P. Kuhns [a], G. Christou [b], N.S. Dalal [a,*]

[a] Department of Chemistry and Biochemistry and National High Magnetic Field Laboratory, Florida State University, Tallahassee, FL 32306, USA
[b] Department of Chemistry, University of Florida, Gainesville, FL 32611, USA

Received 5 October 2004; accepted 24 October 2004
Available online 15 July 2005

Abstract

X-ray structural, magnetization and ^{55}Mn single crystal NMR investigations of $Mn_{12}O_{12}(CH_2BrCOO)_{16}(4H_2O)\cdot 4CH_2Cl_2$ indicate that this highly symmetric ($I\bar{4}$) lattice, devoid of hydrogen bonding of the Mn_{12}-framework with the molecules of lattice hydration, might be an improved model for studying single-molecule magnetism. Single crystal NMR yield much enhanced NMR data as compared to magnetically oriented powders, enable determination of ^{55}Mn hyperfine and quadrupole couplings, and show that the oriented powder samples do not represent an authentic crystal picture.

Keywords: Single-molecule magnets; ^{55}Mn NMR; Single crystal; Aligned powder

1. Introduction

Single-molecule magnets (SMMs) are currently the subject of many theoretical and experimental investigations because of their surprising property of macroscopic quantum tunneling (MQT) at low temperatures [1]. Novel applications are possible since Mn_{12} and analogs have been proposed as potential materials for elements in quantum computation devices [1,2]. The family of $[Mn_{12}O_{12}(O_2CMe)_{16}(H_2O)_4]\cdot 2MeCO_2H\cdot 4H_2O$, henceforth Mn_{12}–Ac [3], molecules contain an external crown of eight Mn^{3+} ions ($S = 2$), which are ferromagnetically coupled and an inner core of four Mn^{4+} ions ($S = 3/2$), also ferromagnetically coupled. The crown and core are antiferromagnetically coupled to produce a total spin of $S = 10$. The symmetry implies an effective Hamiltonian that is dominated by a strong easy-axis term $H = DS_z^2$, with $D = -0.56$ K, which splits the ground state such that the degenerate $m_s = \pm 10$ levels lie lowest. The fundamental question in this material so far concerns the nature of the basic mechanism underlying the MQT behavior. According to theory, MQT may be induced by fourth order transverse anisotropy, phonons effect, or dipolar interactions with dynamic hyperfine fields. Indeed, electron paramagnetic resonance [4–13] (EPR) and inelastic neutron scattering [14–17] experiments have shown the presence of a fourth order transverse anisotropy term $[S_4^+ + S_4^-]$ in the spin Hamiltonian, however, this term cannot account for the observed odd tunneling resonances in magnetic relaxation. Besides, hyperfine and dipolar interactions are too weak to provide the actual tunneling rates. Recently, based on a detailed X-ray analysis, Cornia et al. [18] have suggested that the solvated molecules play a crucial role in the mechanism of the MQT phenomena, via strong hydrogen-bonding and

* Corresponding author. Tel.: +1 850 6443398; fax: +1 850 6443810.
E-mail addresses: aharter@chem.fsu.edu (A.G. Harter), dalal@chemmail.chem.fsu.edu (N.S. Dalal).

0277-5387/$ - see front matter © 2005 Published by Elsevier Ltd.
doi:10.1016/j.poly.2005.03.117

thus the lowering of the lattice symmetry, and the presence of the rhombic (E) term in the spin Hamiltonian. It is thus of interest to examine, by solid state NMR spectroscopy, the role of the lattice-solvated molecules in the overall magnetic symmetry and structure of Mn_{12}–Ac and related compounds. To this effect, we have carried out ^{55}Mn NMR measurements on the recently synthesized compound $[Mn_{12}O_{12}(O_2CCH_2Br)_{16}(H_2O)_4]\cdot 4CH_2Cl_2$ (Fig. 1), henceforth as Mn_{12}–BrAc [19]. In particular, we examined the NMR spectra of single crystal as well as aligned powder of this compound. We found significant differences between the spectra from the single crystals versus aligned powder; specifically that the single crystals afford significantly higher spectral resolution than the aligned powder, and moreover, that the act of powdering introduces significant differences in the chemical structure of Mn_{12}–BrAc. Furthermore, angular dependence studies are now possible because of the use of single crystals. We conducted such studies with rotations in the *ac*-plane.

2. Synthesis and crystal growth

Mn_{12}–BrAc was synthesized by mixing Mn_{12}–Ac in toluene and then adding an excess of HO_2CCH_2Br, as described elsewhere [19]. Once the initial crystals of Mn_{12}–BrAc were formed, they were recrystallized by dissolving in dichloromethane and adding bromoacetic acid. Once dissolved, the solution was filtered and placed into small vials with a small amount of hexanes. A needle was pushed through the lid to assure slow evaporation. After a week, nice brick looking single crystals form.

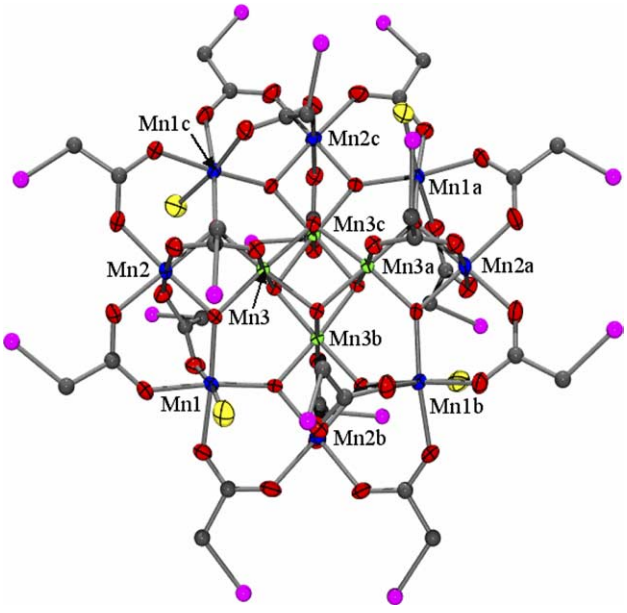

Fig. 1. ORTEP representation in PovRay format of Mn_{12}–BrAc.

3. NMR experimental details

^{55}Mn NMR measurements were made using a home built MAGRes2000 Integrated Wideband NMR spectrometer with quadrature detection and a home built high frequency probe [20,21]. The crystal samples were prepared by removing the crystal from its mother liquor and immediately covering in 5-min epoxy to prevent the sample from drying. Immediately after the epoxy was set, the sample was mounted into the coil and cooled in a dewar of liquid Helium. Aligned powder samples were made by crushing the crystals and then mixing with Stycast 1266 epoxy. On crushing the sample, it was noticed that the crystals went from a dark wet looking brown color to a light brown, dry powdery sample. The epoxy was then allowed to cure overnight at room temperature in a field of 8.5 T. Data was acquired for both samples at ~2 K, below the blocking temperature, T_B, of ~3 K because of fast T_2 times above this temperature. A Hahn echo pulse sequence was used while the frequency was scanned from 220 to 400 MHz, usually taking 0.1–0.2 MHz steps. Frequency scans were necessary because of the large peak widths (~5–20 MHz). Pulse lengths were on the order of hundreds of nanoseconds giving a bandwidth of roughly ~2 MHz. After the scan, the data was processed using a Fast Fourier Transform Sum (FFT Sum).

4. Results

We present here the comparison of single crystal ^{55}Mn NMR spectroscopic measurements of $[Mn_{12}O_{12}(O_2CCH_2Br)_{16}(H_2O)_4]\cdot 4CH_2Cl_2$ (Fig. 2, henceforth Mn_{12}–BrAc) and an aligned powder sample of Mn_{12}–BrAc. As will be seen, the ability to probe Mn sites represents a powerful tool to study factors such as symmetry-lower-

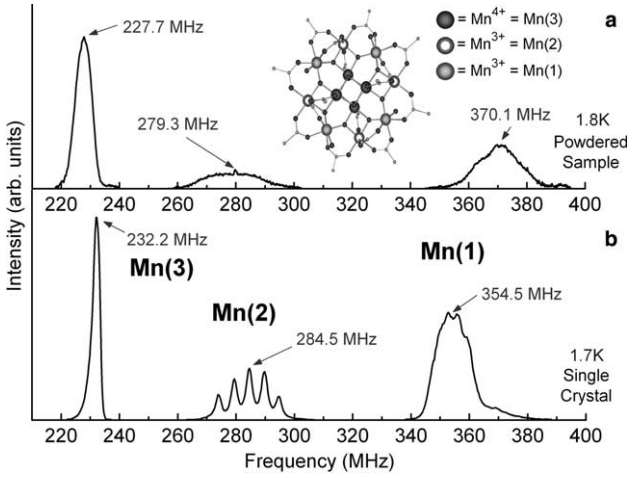

Fig. 2. Comparison of Mn_{12}–BrAc aligned powder vs. single crystal. Inset shows the core crystal structure and assigns the peaks.

ing in SMMs due to extrinsic perturbations and the ground state at each Mn ion. Mn_{12}–BrAc yield large single crystals suitable for ^{55}Mn NMR studies. Fig. 2 shows a comparison of ^{55}Mn NMR signals obtained from: (a) Mn_{12}–BrAc powder and (b) a Mn_{12}–BrAc single crystal, all in zero external field, $H_0 = 0$.

The aligned powder spectrum of Mn_{12}–BrAc, Fig. 2(a), shows three peaks corresponding to the three expected sites of the Mn ions [22,23]. The first peak (Mn(3)) at 227.7 MHz corresponds to the Mn^{4+} ions in the Mn_4O_4 core and has Full Width at Half Maximum (FWHM) of 6.52 MHz. The second peak (Mn(2)) at 279.3 MHz, with a FWHM of 24.74 MHz, is a result of four of the Mn^{3+} ions located in the crown of the molecule. No quadrupolar splitting is noticed. The last four Mn^{3+} ions located in the crown of the molecule produce the third peak (Mn(1)) at 370.1 MHz and a FWHM of 16.67 MHz. Again, no quadrupolar information can be extracted from this peak. Hyperfine fields can be calculated by using $\gamma_n^{55} = 10.5$ MHz/T resulting in fields of 21.69, 26.60, and 35.25 T corresponding to Mn(3), Mn(2), and Mn(1), respectively.

Upon examining the single crystal data (Fig. 2(b)) a sharp distinction is noticed. Resolution is far superior to that of the aligned powder and the peaks are actually shifted, up to ~16 MHz. The peak assignments are the same as the aligned powder. The narrow first peak has a frequency of 232.2 MHz, a FWHM of 2.89 MHz, and a hyperfine field of 22.11 T. The second quadrupolar split line has a central transition at 284.5 MHz, a FWHM of 2.91 MHz and an internal field of 27.10 T. Lastly, the third peak occurs at 354.5 MHz with a hyperfine field of 33.76 T. While the resolution is not great enough to measure the width of one of the quadrupolar split peaks, the FWHM for the entire peak is 13.82 MHz. All data should be contrasted with that obtained from the aligned powder.

The large resolution enhancement afforded by use of single crystals allows us to calculate the quadrupole coupling parameter e^2qQ for the second and third peaks through the quadrupole splitting, $\Delta\nu_Q$, and the equation for the energy [22,23]

$$\mathbf{E}_m = -\gamma_n \hbar H_0 m + \frac{e^2qQ}{4I(2I-1)}\left(\frac{3\cos^2\theta - 1}{2}\right)[3m^2 - I(I+1)],$$

where I and m are the nuclear spin and its projection quantum numbers, and θ the angle from the symmetry axis. From crystallographic data for Mn_{12}–BrAc, it is known that the local Jahn–Teller axes, and hence the principal hyperfine field directions of Mn(2) and Mn(1) ions are canted away from the c-axis at angles of 7.9° and 34.0°, respectively. With $I = 5/2$, $\Delta\nu_Q = 5.15 \pm 0.05$ MHz for the Mn(2) peak while $\Delta\nu_Q = 3.3 \pm 0.10$ MHz for the Mn(1) peak resulting in e^2qQ values of 35.33 ± 0.35 and 41.43 ± 1.26 MHz, respectively. No such information is obtainable from the oriented powder data (Fig. 2(a)).

Powdering the sample obviously changes the environment of the Mn ions, most likely due to the pressure and temperature change placed on the crystals when they are crushed. Further studies of these effects are underway to determine the exact cause of the transformation. More significant to this work is the knowledge that an aligned powder does not represent a statistical average of the crystal, as is seen by the large shift of the peaks in the aligned powdered spectra. It is thus suggested that work on aligned powders should be viewed with caution.

Yet another advantage to using single crystals is the ability to perform angular dependence studies. Angular dependence of the Mn(3) peak of Mn_{12}–BrAc was conducted from the easy to hard axis, as shown in Fig. 3. Rotation in the ac plane was prepared by cooling the crystal in zero field, so signals from both $m_s = \pm 10$ states are discernible, separated by twice the Zeeman frequency at the applied field (1 T here). The angular variation in the *ac*-plane is described by the following equation:

$$\textit{Peak Frequency} = \nu_{CF} \pm (^{55}\gamma/2\pi)(H_0)(\cos\theta).$$

ν_{CF} represents the central frequency and θ being the angle between H_0 and the c-axis. As the crystal is rotated, the effective field, H_{eff}, felt by the nuclei is just the sum of the projection of H_0 onto the hyperfine field, H_N ($H_{eff} = H_N \pm H_0\cos\theta$). Thus, a maximum in the splitting is seen when H_0 is parallel to the c-axis ($\theta = 0°$) while a minimum in the splitting is noticed when H_0 is perpendicular to the c-axis ($\theta = 90°$). One interesting result is the splitting observed when the crystallographic c-axis is perpendicular to the external field, H_0. When the crystal is in this configuration and an external field is applied, we observe two peaks as opposed to the expected one. We tentatively assign this to two different orientations of the hyperfine fields at the Mn^{4+} sites.

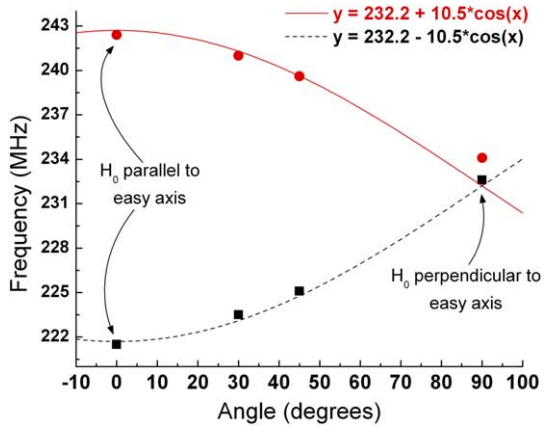

Fig. 3. Angular dependence in the *ac*-plane of a single crystal of Mn_{12}–BrAc.

5. Conclusion

Loss of information from aligned powdered samples is obvious by the shifts in frequency and loss of quadrupolar splitting. Single crystal measurements offer a new way to probe the magnetic properties of SMM by providing more accurate measurements of hyperfine fields and quadrupolar information. Angular dependence studies show that there is more work to be done to understand the magnetic structure of this molecule. The higher symmetry of Mn_{12}–BrAc, as a result of having no waters of hydration to allow hydrogen bonding, produces a less convoluted spectrum than Mn_{12}–Ac, suggesting that Mn_{12}–BrAc is a model system to study for understanding magnetic tunneling in the Mn_{12} family. Two recent studies [24–26] support this conclusion.

Acknowledgement

This work was supported by the NSF-DMR Grant # DMR 0103290.

References

[1] G. Christou, D. Gatteschi, D.N. Hendrickson, MRS Bulletin 25 (2000) 66.
[2] D. Gatteschi, R. Sessoli, Angew. Chem. Int. Ed. Eng 42 (2003) 26.
[3] T. Lis, Acta Crystallogrr. B36 (1980) 2042.
[4] S. Hill, J.A.A.J. Perenboom, N.S. Dalal, T. Hathaway, T. Stalcup, J.S. Brooks, Phys. Rev. Lett. 80 (1998) 2453.
[5] J.A.A.J. Perenboom, J.S. Brooks, S. Hill, T. Hathaway, N.S. Dalal, Phys. Rev. B 58 (1998) 330.
[6] S. Hill, S. Maccagnano, K. Park, R.M. Achey, J.M. North, N.S. Dalal, Phys. Rev. B 65 (2002) 224410.
[7] A. Mukhin, V.D. Travkin, A.K. Zvezdin, S.P. Lebedev, A. Caneschi, D. Gatteschi, Europhys. Lett. 44 (1998) 778.
[8] A. Mukhin, B. Gorshunov, M. Dressel, C. Sangregorio, D. Gatteschi, Phys. Rev. B 63 (2001) 214411.
[9] M. Dressel, B. Gorshunov, K. Rajagopal, S. Vongtragool, A.A. Mukhin, Phys. Rev. B 67 (2003) 060405.
[10] A.L. Barra, D. Gatteschi, R. Sessoli, Phys. Rev. B 56 (1997) 8192.
[11] R. Blinc, P. Cevc, D. Arcon, N.S. Dalal, R.M. Achey, Phys Rev. B 63 (2001) 212401.
[12] K. Park, M.A. Novotny, N.S. Dalal, S. Hill, P.A. Rikvold, Phys. Rev. B 65 (2002) 014426.
[13] K. Park, M.A. Novotny, N.S. Dalal, S. Hill, P.A. Rikvold, J. Appl. Phys. 91 (2002) 7167.
[14] S. Carretta, E. Liviotti, G. Amoretti, R. Caciuffo, A. Caneschi, D. Gatteschi, Phys. Rev. B 65 (2002) 052411.
[15] M. Hennion, L. Pardi, I. Mirebeau, E. Suard, R. Sessoli, A. Caneschi, Phys. Rev. B 56 (1997) 8819.
[16] I. Mirebeau, M. Hennion, H. Casalta, H. Andres, H.U. Gudel, A.V. Irodova, A. Caneschi, Phys. Rev. Lett. 83 (1999) 628.
[17] R. Caciuffo, G. Amoretti, A. Murani, R. Sessoli, A. Caneschi, D. Gatteschi, Phys. Rev. Lett. 81 (1998) 4744.
[18] A. Cornia, R. Sessoli, L. Sorace, D. Gatteschi, A.L. Barra, C. Daiguebonne, Phys. Rev. Lett. 89 (2002) 257201.
[19] H. Tsai, D. Chen, C. Yang, T. Jwo, C. Wur, G. Lee, Y. Wang, Inorg. Chem. Commun. 4 (2001) 511.
[20] R.M. Achey, P.L. Kuhns, A.P. Reyes, W.G. Moulton, N.S. Dalal, Phys. Rev. B 64 (2001) 064420.
[21] R.M. Achey, P.L. Kuhns, A.P. Reyes, W.G. Moulton, N.S. Dalal, Solid-State Commun. 121 (2002) 107.
[22] T. Kubo, T. Goto, T. Koshiba, K. Takeda, K. Awaga, Phys. Rev. B 65 (2002) 224425.
[23] Y. Furukawa, K. Watanabe, K. Kumagai, F. Borsa, T. Sasaki, N. Kobayashi, D. Gatteschi, Phys. Rev. B 67 (2003) 064426.
[24] A.G. Harter, N.E. Chakov, B. Roberts, R. Achey, A. Reyes, P. Kuhns, G. Christou, N.S. Dalal, Inorg. Chem. 44 (2005) 2122.
[25] S. Hill, R.S. Edwards, S.I. Jones, N.S. Dalal, J.M. North, Phys. Rev. Lett. 90 (2003) 217204.
[26] E. del Barco, A.D. Kent, E.M. Rumberger, D.N. Hendrickson, G. Christou, Phys. Rev. Lett. 91 (2003) 047203.